Performance Analysis of a Thermionic Thermal Detector at 400K, 300K, and 200K*

by
Darin Leahy, Melanie Weeks, Prahba Tedrow**, James E. Murguia**
AFRL/SNHI Hanscom AFB, Bedford MA 01731
Solid State Scientific Corporation 27-2 Wright Road Hollis NH 03049**

Abstract

The Thermionic Thermal Detector (TTD) is a silicon Schottky diode LWIR infrared sensing element whose operation is not related to classic photoemissive Schottky diode photon detectors. The TTD operates with the individual elements thermally isolated (as in a microbolometer), and uses a reverse bias Schottky diode as the thermal sensing element. The Schottky diode is thermally modulated and the reverse bias current is measured. For a fixed bias voltage and Schottky barrier height, the magnitude of the reverse bias current from the diode is a measure of the diode temperature. Experimental Schottky barrier heights were determined using Richardson activation energy plots. The reverse bias current in a Schottky diode is exponentially dependent on the temperature of the detector, it has a high temperature coefficient 6%/K, at room temperature. The operating temperature of the detector is designed into the device by selecting a metal with the appropriate Schottky barrier height. An array of silicon based Schottky diodes is highly uniform, has no 1/f noise, provides a high impedance source to the multiplexer, and is 100% silicon processing compatible.

This paper describes the theoretical performance of an LWIR sensor based on a state of the art microbolometer multiplexer, using the TTD as the sensing element. The analysis models the detector using the appropriate optical radiation, thermal diffusion, and electrical conduction equations for 400K, 300K, and 200K operation using three different metal silicides. The effects of the optical radiation noise, thermal diffusion noise, detector Johnson noise, detector shot noise, and amplifier noise are considered in the analysis. Samples of the TTD designed for operation at 300K, and suitable for integration with a multiplexer, were fabricated and electrically tested. Thus, the predicted NEDT of an uncooled sensor based on a TTD LWIR thermal sensing element is 6mK.

1. Introduction

Under the sponsorship of the Defense Advanced Research Projects Agency (DARPA), Air Force Research Laboratory (AFRL) at Hanscom AFB and Solid State Scientific Corporation (SSSC) have developed the theory of operation for the Thermionic Thermal Detector (TTD) for uncooled infrared sensing of 8 to 14 μm radiation based on a Schottky diode sensing element. In addition, sample detectors have been fabricated with electrical characteristics that correspond to an NEDT of 6 mK if integrated with a state of the art microbolometer multiplexer.

The standard construction for a microbolometer consists of a thin film VO_x resistor suspended on a thermally isolating membrane, as shown in Fig. 1. The detector temperature is sampled with a current, and the current is compared to a that of a reference detector that is not exposed to the LWIR radiation. The difference in the currents is the signal. The thermally sensitive element in the bolometer is vanadium oxide (VO_x). VO_x has a temperature coefficient of 2 %/K, that is, the resistance of a VO_x film changes by 2% for every 1 °C change in the temperature of the film. The LWIR radiation from a 300 K source typically raises the temperature of the detector film by only 10-20 mK at F/1; consequently, the sample current must be large enough to produce the required sensitivity when it is scaled by the temperature coefficient of the film, and the small temperature rise of the film. The sample current is typically limited to approximately 150 μA by the power handling capability of the VO_x, corresponding to a sample charge of approximately 10 billion electrons.

The thermionic thermal detector is a new type of device whose operation is not related to classic photo-

* This work was supported by the Defense Advanced Research Projects Agency and the Air Force Research Laboratory Sensors Directorate

REPORT DOCUMENTATION PAGE

Form Approved OMB No. 0704-0188

1. REPORT DATE (DD-MM-YYYY)	2. REPORT TYPE	3. DATES COVERED (FROM - TO)
01-01-1998	Conference Proceedings	xx-xx-1998 to xx-xx-1998

4. TITLE AND SUBTITLE
Performance Analysis of a Thermionic Thermal Detector at 400K, 300K, and 200K
Unclassified

5a. CONTRACT NUMBER
5b. GRANT NUMBER
5c. PROGRAM ELEMENT NUMBER

6. AUTHOR(S)
Leahy, Darin ;
Weeks, Melanie ;
Tedrow, Prahba ;
Murguia, James E. ;

5d. PROJECT NUMBER
5e. TASK NUMBER
5f. WORK UNIT NUMBER

7. PERFORMING ORGANIZATION NAME AND ADDRESS
AFRL/SNHI
Hanscom AFB
Bedford, MA01731

8. PERFORMING ORGANIZATION REPORT NUMBER

9. SPONSORING/MONITORING AGENCY NAME AND ADDRESS
Director, CECOM RDEC
Night Vision and Electronic Sensors Directorate
10221 Burbeck Road
Ft. Belvoir, VA22060-5806

10. SPONSOR/MONITOR'S ACRONYM(S)
11. SPONSOR/MONITOR'S REPORT NUMBER(S)

12. DISTRIBUTION/AVAILABILITY STATEMENT
APUBLIC RELEASE
,

13. SUPPLEMENTARY NOTES
See Also ADM201041, 1998 IRIS Proceedings on CD-ROM.

14. ABSTRACT
The Thermionic Thermal Detector (TTD) is a silicon Schottky diode LWIR infrared sensing element whose operation is not related to classic photoemissive Schottky diode photon detectors. The TTD operates with the individual elements thermally isolated (as in a microbolometer), and uses a reverse bias Schottky diode as the thermal sensing element. The Schottky diode is thermally modulated and the reverse bias current is measured. For a fixed bias voltage and Schottky barrier height, the magnitude of the reverse bias current from the diode is a measure of the diode temperature. Experimental Schottky barrier heights were determined using Richardson activation energy plots. The reverse bias current in a Schottky diode is exponentially dependent on the temperature of the detector, it has a high temperature coefficient 6%/K, at room temperature. The operating temperature of the detector is designed into the device by selecting a metal with the appropriate Schottky barrier height. An array of silicon based Schottky diodes is highly uniform, has no 1/f noise, provides a high impedance source to the multiplexer, and is 100% silicon processing compatible. This paper describes the theoretical performance of an LWIR sensor based on a state of the art microbolometer multiplexer, using the TTD as the sensing element. The analysis models the detector using the appropriate optical radiation, thermal diffusion, and electrical conduction equations for 400K, 300K, and 200K operation using three different metal silicides. The effects of the optical radiation noise, thermal diffusion noise, detector Johnson noise, detector shot noise, and amplifier noise are considered in the analysis. Samples of the TTD designed for operation at 300K, and suitable for integration with a multiplexer, were fabricated and electrically tested. Thus, the predicted NEDT of an uncooled sensor based on a TTD LWIR thermal sensing element is 6mK.

15. SUBJECT TERMS

16. SECURITY CLASSIFICATION OF:			17. LIMITATION OF ABSTRACT	18. NUMBER OF PAGES	19. NAME OF RESPONSIBLE PERSON
a. REPORT	b. ABSTRACT	c. THIS PAGE	Public Release	17	Fenster, Lynn lfenster@dtic.mil
Unclassified	Unclassified	Unclassified			19b. TELEPHONE NUMBER International Area Code Area Code Telephone Number 703767-9007 DSN 427-9007

emissive Schottky diode photon detectors. The TTD operate with the individual elements thermally isolated and uses a reverse bias Schottky diode as the sensing element. For a fixed bias voltage and Schottky barrier height, the magnitude of the reverse bias current from the diode is a measure of the diode temperature.

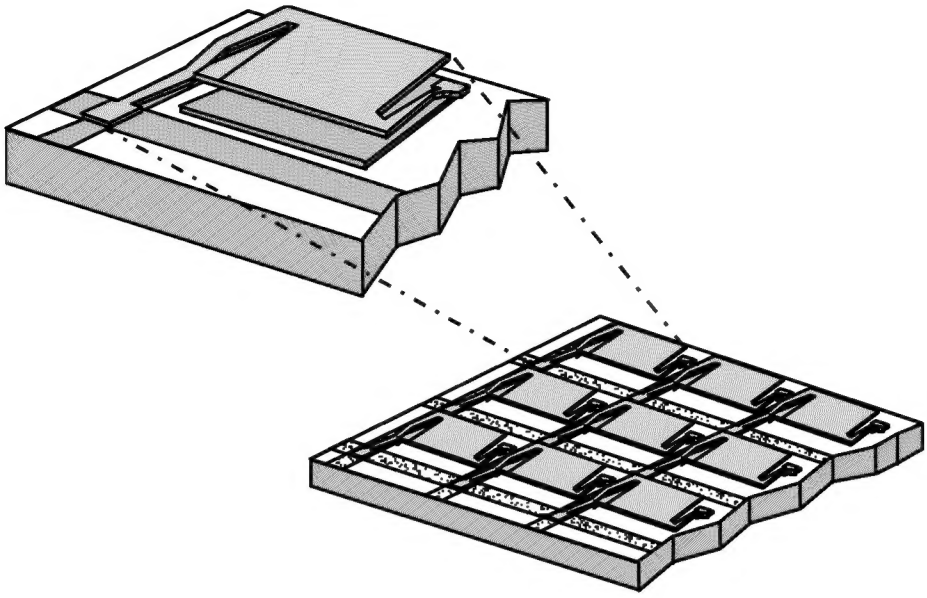

Fig. 1: VO_x resistor based microbolometer, suspended on a thermally isolating membrane.

Central to the development of the thermionic thermal detector is the maturation of three key microelectronic technologies; the fabrication of high ideality metal-semiconductor Schottky diodes with a variety of various barrier heights,[1] the micromachining of thermally isolated silicon microstructure arrays,[2,3,4] and the availability of high quality SIMOX and BESOI wafers.[5]

The TTD has a number of attractive characteristics, namely,

- High sensitivity of output signal current to temperature, **6%/K**.
- A theoretical NEDT of **6 mK** for a 50x50 μm^2 detector element operating at room temperature with a 0.36 eV barrier in the 8-14 mm band at 30 Hz. frame rate and F/1 optics.
- Low temporal noise and no measurable 1/F noise, the same characteristics found in Schottky photon detectors.
- Low spatial nonuniformity and pattern noise, as found in metal Schottky photon detectors.
- High quality low leakage Schottky diode temperature sensing element with good thermal isolation, and no crosstalk when fabricated on SOI.
- 100% compatible with conventional silicon CMOS manufacturing.

The subsequent sections describe the operation of the TTD in terms of the fundamental equations that govern its operation. Tables 1-2 define parameters used in the following development. Sections two through four provide a detailed description of the applicable optical, thermal and electrical equations that govern the operation of the TTD device element. Section five illustrates the affect of the multiplexer on the array. Section six defines the noise equivalent temperature (NEDT) of the array in terms of the equations derived in the previous sections. Performance calculations and graphs that refer to the TTD use the definition for NEDT in Eq. 6.6, with the noise term given by Eq. 6.3. Additional simplifications described in section six are used to provide insight into the operation of the TTD. Finally, performance calculations for the TTD based on the above model are described in section 7.

q	=	1.602×10^{-19} C	Charge on an electron.
A^{**}	=	30 $A \cdot cm^{-2} \cdot K^{-2}$	Richardson's Constant (p-type Si)
k	=	1.383×10^{-23} $J \cdot K^{-1}$	Boltzmann's constant.
ε_{si}	=	1.054×10^{-12} $F \cdot cm^{-2}$	Dielectric constant of Si.
ε_{ox}	=	3.45×10^{-13} $F \cdot cm^{-2}$	Dielectric constant of thermal SiO_2.
π	=	3.14159	Value of Pi.
σ	=	5.67×10^{-12} $W \cdot cm^{-2} \cdot K^{-4}$	Stefan-Boltzmann constant.

Table 1: Constants used in TTD analysis.

R_{Diff}	$K \cdot W^{-1}$	Thermal resistance due to diffusion.
G_{Diff}	$W \cdot K^{-1}$	Thermal Diffusive Conductance.
G_{Rad}	$W \cdot K^{-1}$	Thermal Radiative Conductance.
R_{Teq}	$K \cdot W^{-1}$	Thermal resistance due to diffusion and radiation.
κ	$W \cdot K^{-1}$	Thermal Conductance of Schottky diode.
C_{Therm}	$J \cdot K^{-1}$	Thermal heat capacitance of pixel.
Q_{Rad}	W	Heat radiated from detector.
Q_B	W	Heat radiated from background.
Q_S	W	Heat radiated from signal.
Q_{Bias}	W	Heat generated from bias.
Q_{Diff}	W	Heat transferred by diffusion.
P_S	W	Power radiated from signal.
P_B	W	Power radiated from background.
P_{Rad}	W	Power radiated from detector.
P_D	W	Power radiated on detector.
P_{DS}	W	Power radiated on detector from signal.
P_{DB}	W	Power radiated on detector from background.
T_S	K	Temperature of scene.
T_B	K	Temperature of background.
T_D	K	Temperature of detector.
$f_{\#}$		F number of system.
ε_D		Emissivity of Detector.
ε_S		Emissivity of Target.
ε_B		Emissivity of Background.
V	V	Applied Bias Voltage on Schottky Diode.
N_D	cm^{-3}	Impurity concentration of p-type dopants.
N_C	cm^{-3}	Density of states in Si conduction band.
ψ_o	eV	Schottky barrier height (0.42 eV for $CoSi_2$ on lightly doped p-type Si @ V=0).
A_{Eff}	cm^{-2}	Detector effective active area (1.5×10^{-5} cm^2 is 60% of 50x50 μm^2 pixel)
R_{Det}	Ω	Electrical resistance of detector (large signal)
R_{det}	Ω	Electrical resistance of detector (small signal)
R_F	Ω	Feedback resistance on amplifier.
R_L	Ω	Load resistance on amplifier.
Frame	s^{-1}	Frame rate.
S		Number of stages or pixels/column.
v_{na}	V	Input referred voltage noise of amplifier.

Table 2: Variables used in TTD analysis.

2. Optical Radiation Equations

The heat flow from the surface of the detector via radiation follows the Stefan-Boltzmann law, namely,

$$P_{Rad} = A_{Eff}\varepsilon_D\sigma T_D^4. \tag{2.1}$$

where the thermal conductance of the detector due to radiation, G_{Rad}, is given by,[6]

$$G_{Rad} = 4A_{Eff}\varepsilon_D\sigma T^3. \tag{2.2}$$

In Eq. 2.2, the detector pixel is approximated by a thin flat plate that radiates in the forward direction, and is assumed to be Lambertian. Eq. 2.2 is also derived in Section 3. The optical power on a detector is the sum of the signal power and the background power,

$$P_D = P_{DS} + P_{DB} = \frac{A_{Eff}\varepsilon_D\sigma T_S^4}{(2f_{\#})^2+1} + (1-\frac{1}{(2f_{\#})^2+1})A_{Eff}\varepsilon_D\sigma T_B^4. \tag{2.3}$$

The emissivity of the background and the source is assumed to be one. Differentiating Eq. 2.3, the change in power on a detector for an incremental change in signal temperature is given by,

$$\frac{dP_D}{dT_S} = \frac{dP_{DS}}{dT_S} = \frac{4A_{Eff}\varepsilon_D\sigma T_S^3}{(2f_{\#})^2+1}. \tag{2.4}$$

The radiation noise in a TTD is given by the noise equivalent power (NEP) due to radiation noise [1]

$$< NEP_{Rad} >^2 = 4kT^2BG_{Rad}. \tag{2.5}$$

3. Thermal Diffusion Equations

The heat flow equation for the temperature of the detector, T_D, is given by,

$$\rho c_s\frac{\partial T_D}{\partial t} = \kappa\left(\frac{\partial^2 T_D}{\partial x^2}+\frac{\partial^2 T_D}{\partial y^2}+\frac{\partial^2 T_D}{\partial z^2}\right) - Q_{Rad}^{out} + Q_B^{in} + Q_S^{in} + Q_{Bias}^{in} - Q_{Diff}^{out} \tag{3.1}$$

where κ is the thermal conductivity of the Schottky diode, ρ is the mass density, c_s is the specific heat, and Q is the heat flow due to pixel radiation, image background temperature, image scene temperature, diode bias, and thermal diffusion, respectively. A uniformly illuminated square pixel with a high thermal conductivity has a spatially uniform temperature distribution that can be approximated by,

$$\rho c_s\frac{\partial \Delta T_D}{\partial t} = -Q_{Rad}^{out} + Q_B^{in} + Q_S^{in} + Q_{Bias}^{in} - Q_{Diff}^{out}, \tag{3.2}$$

where ΔT_D is the temperature difference between the background and the detector pixel. In steady state, $\partial\Delta T_D/\partial t = 0$, and the power emitted from the detector is equal to the power on the detector,

$$Q_{Rad}^{out} + Q_{Diff}^{out} = Q_B^{in} + Q_S^{in} + Q_{Bias}^{in} = P_{DS} + P_{DB} + Q_{Bias}^{in}. \tag{3.3}$$

For a pixel of area A_{Eff},

$$A_{Eff}\varepsilon_D\sigma T_D^4 + \frac{(T_D - T_B)}{R_{Diff}} = \frac{A_{Eff}\varepsilon_D\sigma T_S^4}{(2f_{\#})^2 + 1} + (1 - \frac{1}{(2f_{\#})^2 + 1})A_{Eff}\varepsilon_D\sigma T_B^4 + VI_{Bias} \qquad 3.4$$

where the terms correspond to the power radiated by the detector, the power thermally diffused from the pixel, the power radiated from the small signal onto the pixel, the power radiated from the background onto the pixel, and the power injected from the bias current into pixel, respectively.

The power on the detector radiated from a small signal above background is adapted from Eq 2.3,

$$\delta P_{DS} = \frac{A_{Eff}\varepsilon_D\sigma T_S^4}{(2f_{\#})^2 + 1},$$

consequently,

$$A_{Eff}\varepsilon_D\sigma T_D^4 + \frac{(T_D - T_B)}{R_{Diff}} = \delta P_{DS} + (1 - \frac{1}{(2f_{\#})^2 + 1})A_{Eff}\varepsilon_D\sigma T_B^4 + VI_{Bias}. \qquad 3.5$$

Rearranging terms,

$$A_{Eff}\varepsilon_D\sigma T_D^4 - (1 - \frac{1}{(2f_{\#})^2 + 1})A_{Eff}\varepsilon_D\sigma T_B^4 + \frac{(T_D - T_B)}{R_{Diff}} = \delta P_{DS} + VI_{Bias}. \qquad 3.6$$

Applying the operator $\partial/\partial T_D$ on both sides of the equation,

$$4A_{Eff}\varepsilon_D\sigma T_D^3 + R_{Diff}^{-1} = \frac{\delta P_{DS}}{dT_D}, \qquad 3.7$$

or,

$$\frac{dT_D}{\delta P_{DS}} = \frac{dT_D}{dP_{DS}} = \frac{R_{Diff}}{(1 + 4A_{Eff}\varepsilon_D\sigma T_D^3 R_{Diff})}. \qquad 3.8$$

The total equivalent thermal resistance is defined as the parallel combination of the thermal radiation resistance and the thermal diffusion resistance, namely,

$$R_{Teq} = \frac{R_{Diff}R_{Rad}}{R_{Diff} + R_{Rad}}. \qquad 3.9$$

where the thermal radiation resistance is the reciprocal of the thermal radiation conductance, $R_{Rad} = 1/G_{Rad}$,

$$G_{Rad} = 4A_{Eff}\varepsilon_D\sigma T^3. \qquad 3.10$$

The thermal diffusion noise in a TTD is given by the NEP due to diffusion noise [1]

$$< NEP_{Diff} >^2 = 4kT^2 BG_{Diff}, \qquad 3.11$$

where G_{Diff}, the thermal diffusion conductance of the detector. The total thermal noise power is given by the sum of the thermal radiation noise and the thermal diffusion noise,

$$< NEP_{Therm} >^2 = 4kT^2 BG_{Therm}, \tag{3.12}$$

where $G_{Therm} = G_{Rad} + G_{Diff}$. In terms of noise currents, the thermal noise is given by,

$$< i^2_{Therm} >= \frac{4kT^2}{C_{Therm}} \left(\frac{\partial I}{\partial T} \right)^2, \tag{3.13}$$

where C_{Therm} is the thermal capacitance of the pixel. The heat flow due to thermal diffusion from a thermally isolated detector pixel supported by a narrow handle that acts as a thermal heat sink, can be approximated by,

$$Q_{Diff} = \frac{G_{Diff} A_C \Delta T_D}{L}, \tag{3.14}$$

where L is the length of the supporting handle, A_C is the cross sectional area of the supporting handle, and ΔT_D is the temperature difference across the supporting handle.

In zero bias steady state, Eq. 3.4 can be rewritten as,

$$-A_{Eff}\varepsilon_D \sigma T_D^4 + \frac{A_{Eff}\varepsilon_D \sigma T_S^4}{(2f_{\#})^2 + 1} + (1 - \frac{1}{(2f_{\#})^2 + 1}) A_{Eff}\varepsilon_D \sigma T_B^4 - \frac{G_{Diff} A_C \Delta T_D}{L} = 0. \tag{3.15}$$

Expanding in a Taylor series about T_B,

$$\begin{aligned} &-4A_{Eff}\varepsilon_D \sigma T_B^3 (\Delta T_D) + \frac{4A_{Eff}\varepsilon_D \sigma T_B^3 (\Delta T_S)}{(2f_{\#})^2 + 1} \\ &+4(1 - \frac{1}{(2f_{\#})^2 + 1}) A_{Eff}\varepsilon_D \sigma T_B^3 \cdot (0) - \frac{G_{Diff} A_C \Delta T_D}{L} = 0 \end{aligned} \tag{3.16}$$

or,

$$\frac{4A_{Eff}\varepsilon_D \sigma T_B^3 \Delta T_S}{(2F_{\#})^2 + 1} - (4A_{Eff}\varepsilon_D \sigma T_B^3 \Delta T_D) - \frac{G_{Diff} A_C \Delta T_D}{L} = 0. \tag{3.17}$$

The thermal diffusion isolation of a pixel can only be ignored if the radiative heat loss from the pixel is much larger than the diffusive heat loss from the pixel,

$$(4\varepsilon_D \sigma T_B^3 A_{Eff} \Delta T_D) >> \frac{G_{Diff} A_C \Delta T_D}{L} \approx 0. \tag{3.18}$$

The thermal response time of the thermionic thermal detector pixel is given by,

$$\tau = \frac{A_D \rho c_s t_f L}{G_{Diff} A_C}, \tag{3.19}$$

where t_f is the SOI silicon film thickness.

4. Electrical Equations

The current density in a Schottky based thermionic thermal detector is calculated from thermionic emission theory,[7]

$$J = J_S(e^{qV/kT} - 1), \tag{4.1}$$

where kT is the thermal energy, and the saturation current density J_S is given by,

$$J_S = A^{**}T^2 e^{\frac{-q\phi_{bn}}{kT}}. \tag{4.2}$$

In reverse bias, the reverse bias current density reduces to the saturation current density,

$$J_R = J_S = A^{**}T^2 e^{\frac{-q\phi_{bo}}{kT}} e^{\frac{q\sqrt{qE/4\pi\varepsilon_{si}}}{kT}}, \tag{4.3}$$

where $q\phi_{bo}$ is the zero voltage barrier height, E is the electric field, ε_{si} is the dielectric constant of silicon, and A** is the modified Richardson constant. The electric field for an impurity concentration, N, is given by,

$$E = \sqrt{\frac{2qN}{\varepsilon_s}(V + V_{bi} - kT/q)}, \tag{4.4}$$

and reduces the zero voltage barrier height $q\phi_{bo}$, to the effective barrier height, $q\phi_{bn}$, by image force lowering. ϕ_{bn} is given by,

$$\phi_{bn} = \frac{kT}{q}\ln\left(\frac{A^{**}T^2}{J_R}\right) = \phi_{bo} - \sqrt{\frac{qE}{4\pi\varepsilon_{si}}}. \tag{4.5}$$

Barrier lowering can be used to tune the zero voltage Schottky barrier, $q\phi_{bo}$=0.42 eV. Neglecting the small temperature dependence of the electric field in Eq. 4.4, the change in the reverse current in a thermionic detector as a function of temperature, $\partial J_R/\partial T$, is given by,

$$\frac{\partial J_R}{\partial T} = A^{**} e^{\frac{-q\phi_{bo}}{kT}} e^{\frac{q\sqrt{qE/4\pi\varepsilon_{si}}}{kT}}\left[\frac{q\phi_{BO}}{k} - \frac{q\sqrt{qE/4\pi\varepsilon_{si}}}{k}\right] + 2A^{**}Te^{\frac{-q\phi_{bo}}{kT}} e^{\frac{q\sqrt{qE/4\pi\varepsilon_{si}}}{kT}}, \tag{4.6}$$

and represents the sensitivity of the detector to temperature. $(1/J_R)\partial J_R/\partial T$ represents the temperature coefficient of the current in a TTD,

$$\frac{1}{J_R}\frac{\partial J_R}{\partial T} = \left[\frac{q\phi_{BO}}{kT^2} - \frac{q\sqrt{qE/4\pi\varepsilon_{si}}}{kT^2}\right] + \frac{2}{T}. \tag{4.7}$$

For a 0.36 ev schottky barrier on silicon at room temperature, the temperature coefficient, $(1/J_R)\partial J_R/\partial T$, is **6%/K**.

The shot noise in a TTD is given by,

$$< i_{Shot}^2 >= 2qBI_R , \quad 4.8$$

where B is the measurement bandwidth, and I_R is the reverse bias diode current.[8] Assuming the reverse bias is larger than $4kT \cong 0.1V$,

$$I_R \cong A_{Eff} J_S , \quad 4.9$$

and,

$$< i_{Shot}^2 >= 2qBA_{Eff} A^{**} T^2 e^{\frac{-q\phi_{bo}}{kT}} e^{\frac{q\sqrt{qE/4\pi\varepsilon_{si}}}{kT}} . \quad 4.10$$

The Johnson noise in a TTD is given by,

$$< i_{Johnson}^2 >= \frac{4kTB}{R} . \quad 4.11$$

where R is the diode resistance. The differential resistance of the diode can be written as,

$$\frac{1}{R_{det}} = A_{Eff} \frac{\partial J}{\partial V} = A_{Eff} \frac{\partial}{\partial V} J_S (e^{qV/kT} - 1) = \frac{qA_{Eff}}{kT} J_S e^{qV/kT} , \quad 4.12$$

and the large signal resistance of the diode can be written as,

$$R_{Det} = \frac{V}{A_{Eff} J_S} = \frac{V}{A_{Eff} J_S (e^{qV/kT} - 1)} \approx \frac{V}{A_{Eff} J_S} . \quad 4.13$$

The Johnson noise resistance in Eq. 4.11 is a small signal parameter and is given by Eq. 4.12; consequently,

$$< i_{Johnson}^2 >= 4qBAJ_S e^{qV/kT} . \quad 4.14$$

5. Multiplexer and Amplifier

Fig. 2 describes the array architure. Each pixel is composed of a thermally sensitive schottky diode and a row selection transistor. The row select turns on all unit cell transistors in a row to simultaneously bias a detector element in each column. The reverse bias potential of the Schottky diode is determined by the difference between the reference voltage at the diode semiconductor electrode and the the bias potential at the diode metal contact. The metal contact potential is set at each column bus. At the bottom of each column in the array are two transimpedence amplifiers, a differential amplifier, a column select transistor and a thermally insensitive reference pixel. The column bus potential is set by applying the bias potential to the positive input of the transimpedence amplifier. A similar bias potential is applied to the column of the reference pixel for bias current subtraction at the differential amplifier. The transimpedance amplifier converts the detector current to a voltage. The differential amplifier provides differential suppression of DC bias and bias noise, and a programmable integration time. This amplifier is also used to dynamically correct for pixel to pixel nonuniformity in the array.

The column amplifier is similar to one with an output referred voltage noise of approximately 300 μV for a bandwidth of 10 kHz., corresponding to a dynamic range in excess of 10,000:1 (13 bits). The noise voltage gain on the amplifier is 50, consequently, the input referred voltage noise, v_{na}, is 6 μV.

The gain of the amplifier is limited by the dynamic range of the output, and the pixel to pixel nonuniformity of the signal from the array. As the uniformity of the signal from each of the pixels in the array increases, a higher gain differential amplifier can be used without clipping the signal. Newer and higher gain versions of the amplifier can be used on very uniform arrays (i.e. TTD Schottky arrays) with an input referred voltage noise as low as 1.5 μV.

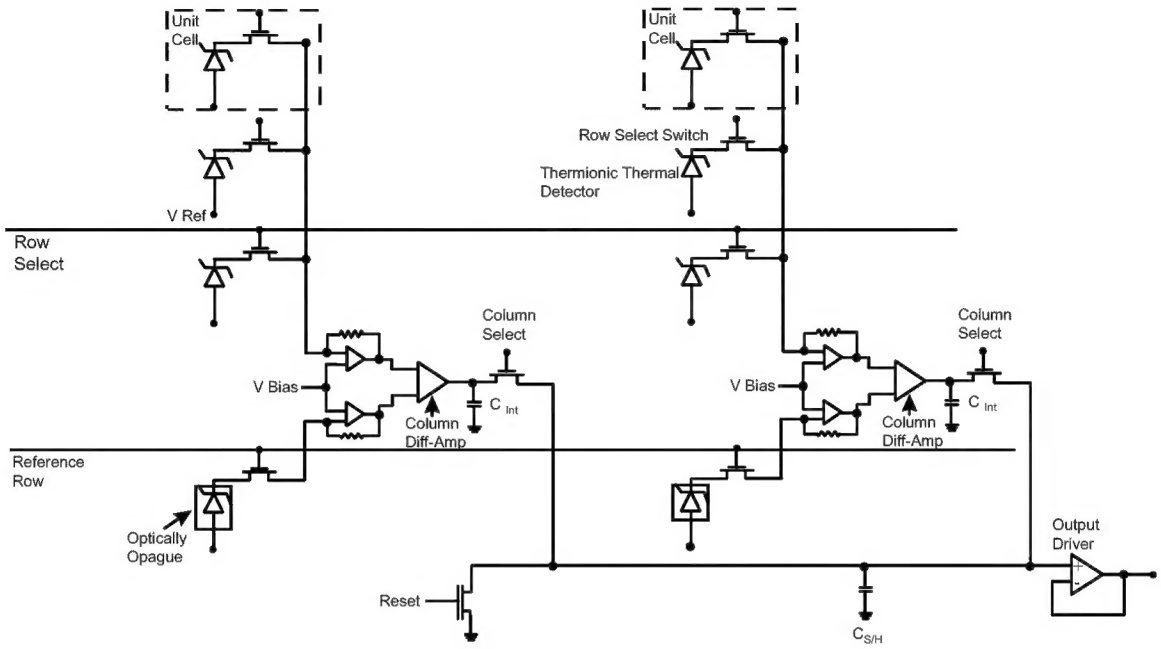

Fig 2: Schematic view of TTD based thermal imaging array

The input current noise of the amplifier, i_{na}, is given by the input referred voltage noise divided by the load resistance to the amplifier, namely,

$$i_{na} = \frac{v_{na}}{R_L} = \frac{v_{na}(R_{det} + R_F)}{R_{det}R_F}, \qquad 5.1$$

with the load resistance given by the parallel combination of the detector resistance and the feedback resistance. Consequently,

$$i_{Amp}^2 = 2\frac{v_{na}^2}{R_L^2} = 2v_{na}^2\frac{(R_{det} + R_F)^2}{(R_{det}R_F)^2}. \qquad 5.2$$

The factor of two arises from the noise of two transimpedance amplifiers in the output multiplexor adding in quadrature. Using the small signal resistance of the TTD as the detector resistance,

$$i_{Amp}^2 = 2v_{na}^2\left(1/R_F + \frac{qA_{Eff}}{kT}J_S e^{qV/kT}\right)^2. \qquad 5.3$$

6. Noise Equivalent Temperature

The total noise in the TTD is given by the quadrature sum of all the contributing noise sources, namely,

$$< i_{Tot}^2 >=< i_{Shot}^2 > + < i_{Johnson}^2 > + < i_{Therm}^2 > + < i_{Amp}^2 >. \quad 6.1$$

where the thermal noise is the sum of the thermal noise due to radiation and the thermal noise due to diffusion. Substituting for each of these terms,

$$< i_{Tot}^2 >= 2qBI + \frac{4kTB}{R} + \frac{4kT^2}{C_{Therm}}\left(\frac{\partial I}{\partial T}\right)^2 + 2v_{na}^2\left(1/R_F + \frac{qA_{Eff}}{kT}J_S\, e^{qV/kT}\right)^2, \quad 6.2$$

or,

$$\begin{aligned} < i_{Tot}^2 >= {} & 2qBA_{Eff}J_S(e^{qV/kT}-1) + 4qBA_{Eff}J_S e^{qV/kT} \\ & + \frac{4kT^2}{C_{Therm}}\left(A_{Eff}J_S(e^{qV/kT}-1)\left[\frac{q\phi_{BO}}{kT^2} - \frac{q\sqrt{qE/4\pi\varepsilon_{si}}}{kT^2}\right] + \frac{2}{T}\right)^2 \\ & + 2v_{na}^2\left(1/R_F + \frac{qA_{Eff}}{kT}J_S\, e^{qV/kT}\right)^2 \end{aligned} \quad 6.3$$

Eq. 6.3 is accurate in the absence of any simplifying approximations describing the magnitude of the applied bias or the relative values of these noise terms. Eq. 6.3 is used to define the noise term in the simulation program TTD-MOD.

At any significant reverse bias above kT (V_{Rev} > 100mV), and with minimal barrier lowering, the diode current can be assumed to be the saturation current. Applying this approximation to Eq. 6.3,

$$\begin{aligned} < i_{Tot}^2 >= {} & 2qBA_{Eff}J_S + 4qBA_{Eff}J_S e^{qV/kT} + \frac{4kT^2}{C_{Therm}}A_{Eff}J_S\left(\frac{q\phi_{BO}}{kT^2} + \frac{2}{T}\right) \\ & + 2v_{na}^2\left(1/R_F + \frac{qA_{Eff}}{kT}J_S\, e^{qV/kT}\right)^2 \end{aligned} \quad 6.4$$

Under reverse bias, the diode resistance is large and the Johnson noise of the diode can be neglected. In addition, the diode resistance term in the amplifier noise is approximately zero. Consequently, Eq. 6.3 reduces to,

$$< i_{Tot}^2 >= 2qBA_{Eff}J_S + \frac{4kT^2}{C_{Therm}}A_{Eff}J_S\left(\frac{q\phi_{BO}}{kT^2} + \frac{2}{T}\right) + 2\frac{v_{na}^2}{R_F^2}. \quad 6.5$$

The NEΔT in a Thermionic Thermal Detector is given by,

$$NE\Delta T = \frac{(T_S - T_B)\sqrt{< i_{Tot}^2 >}}{A_{Eff}J_S(T_D) - A_{Eff}J_S(T_B)}, \quad 6.6$$

where $J_S(T_B)$ is the saturation current through the diode that is imaging the background and $J_S(T_D)$ is the saturation current through the diode that is imaging the target. The diode shot noise current is given by the first term in Eq. 6.5. If the dominant noise in the system is the diode shot noise, and (T_S-T_B) = 1 K, additional approximations can be made to Eq. 6.6, namely,

$$NE\Delta T = \frac{\sqrt{2qBA_{Eff}J_S(T_D)}}{A_{Eff}J_S(T_D) - A_{Eff}J_S(T_B)}. \qquad 6.7$$

7. Performance Calculations of the Thermionic Thermal Detector at 200K, 300K, and 400K

The graphs in Fig. 3 illustrate the performance of the TTD, as described by the above model. The top curve represents the performance of the TTD as a function of the pixel fill factor, using a typical pixel size and a state of the art multiplexer with a thermal conductivity of $5x10^{-8}$ W/K. At a modest 70% fill factor (for a hybrid array), the NEDT of the TTD is predicted to be 6 mK. The bottom curve illustrates the theoretical best performance of the TTD with a thermal conductivity of 10^{-8}

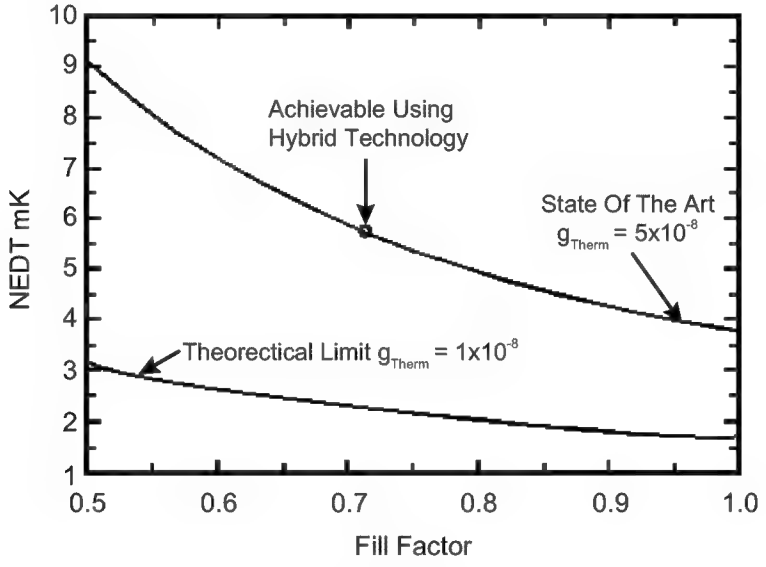

Fig. 3: NEDT performance of a TTD 320x244 array with a 50x50 μm^2 pixel size, 0.36eVbarrier height, $5x10^{-8}$ W/K thermal conductivity, 70 % fill factor, operating in the 8-14 μm band with F/1 optics.

Fig. 4 shows a representative Richardson activation energy plot of a Schottky barrier diode at different reverse biases. This device was fabricated at the Air force Research Laboratory. The substrate was a SIMOX p-type 10-20 ohm-cm wafer with 5.16μm of surface silicon. Further processing was done to define the active area and create an ohmic contact. 10nm of a metal was deposited to form the silicide. The activation energy is obtained by measuring the dark current as a function of temperature with all other current generation mechanisms suppressed. A variety of

different metals and process flows have been used to fabricate devices with barrier heights ranging from 0.22eV to 0.48eV

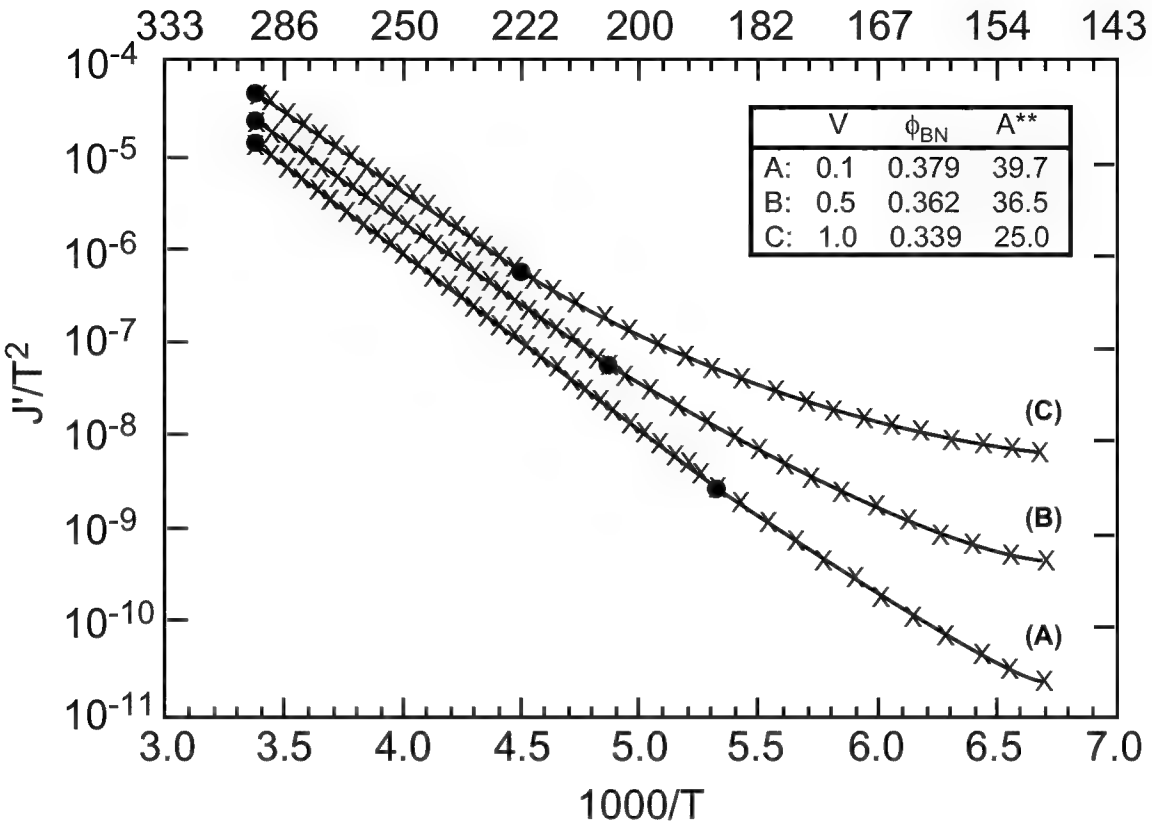

Fig. 4: Richardson curves for a .36 eV Schottky diode fabricated on SOI with a 0.1 V, 0.5 V, and 1.0 V applied reverse bias voltage. The barrier height and Richardson constant are calculated by fitting the curves over 4 orders of magnitude.

In the following analysis, we consider the model for NEDT given by equation 6.3 at three operating temperatures, 200K, 300K, and 400K. These temperatures correspond to different operating environments, namely, space using passive cooling, room temperature uncooled with thermoelectric stabilization, and high temperature with heat stabilization. The theoretical performance demonstrated by Figs. 5,6,7 are of a 320x244 array with a 50x50 μm^2 pixel size, $5x10^{-8}$ W/K thermal conductivity, operating in the 8-14 μm band using F/1 optics at various fill factors. The sample current is typically limited to approximately 150 μA by the power handling capability of the multiplexer, corresponding to a sample charge of approximately 10 billion electrons.

Fig. 5 shows the operation of the TTD at 200K with a 0.23 eV barrier. The graph is of the noise equivalent temperature as a function of F#. It does not consider the effect of cavity cooling thus the graph is understating actual performance. The NEDT of the TTD is predicted to be 4 mK at F/1. The temperature coefficient is 7%/K. total noise

current is 4.19×10^{-19} A and the signal to noise ratio is 15,900. The doping concentration is $3 \times 10^{15} cm^{-3}$ to optimize the current output through image force lowering as can be shown in equation 4.3. This device will be capable of operating in a space environment with only passive cooling techniques.

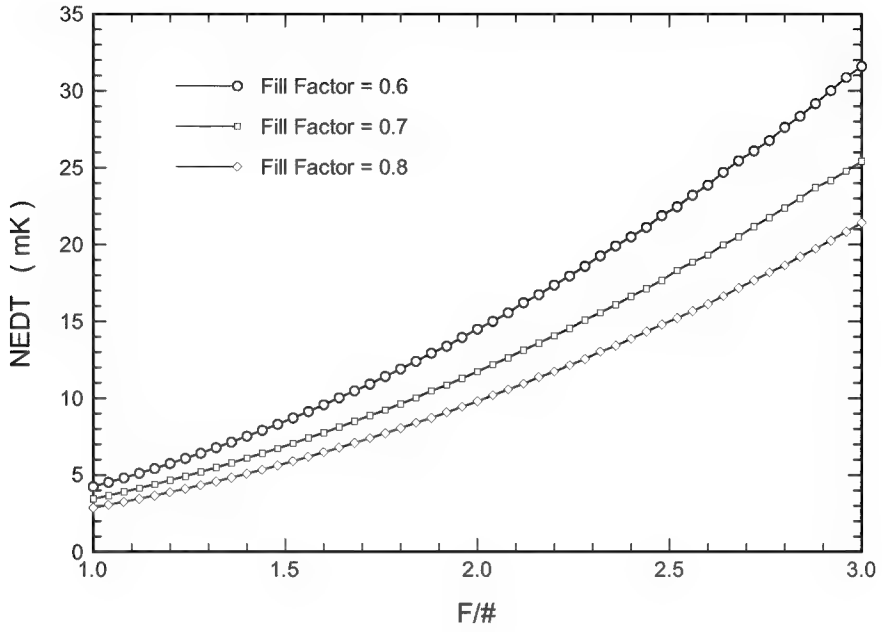

Fig. 5: NEDT performance of a TTD 320x244 array with a 50x50 μm^2 pixel size, 0.23 eV barrier height, 5×10^{-8} W/K thermal conductivity, various fill factors, operating in the 8-14 μm band.

.

Fig. 6: shows the TTD operating at room temperature, 300K, using a 0.36 eV barrier. The NEDT increases to 6mK. The temperature coefficient decreased to 6%K. The total noise current is 4.13×10^{-19} A and the signal to noise ratio is 11,177. The doping concentration is $2 \times 10^{15} cm^{-3}$. The performance of the TTD uncooled is competitive to a microbolometer with vanadium oxide (VO_x) and can be used in the same applications such as maintenance free remote sensing, surveillance and night vision. Temperature stabilization can be achieved by thermoelectric

techniques using substantially less power, due to the IV power consumed by a diode type device as compared to power consumed by a resistive type element. For example consider two devices operating at 300 K. The biasing required for the microbolometer is greater than 2 volts compared to the biasing required for the diode, 4KT or approximately 100mv. In this analysis the diode biasing is 0.5v. The power required for a (VO_x) microbolometer is 325μw compared to 75μw for a Schottky barrier diode.

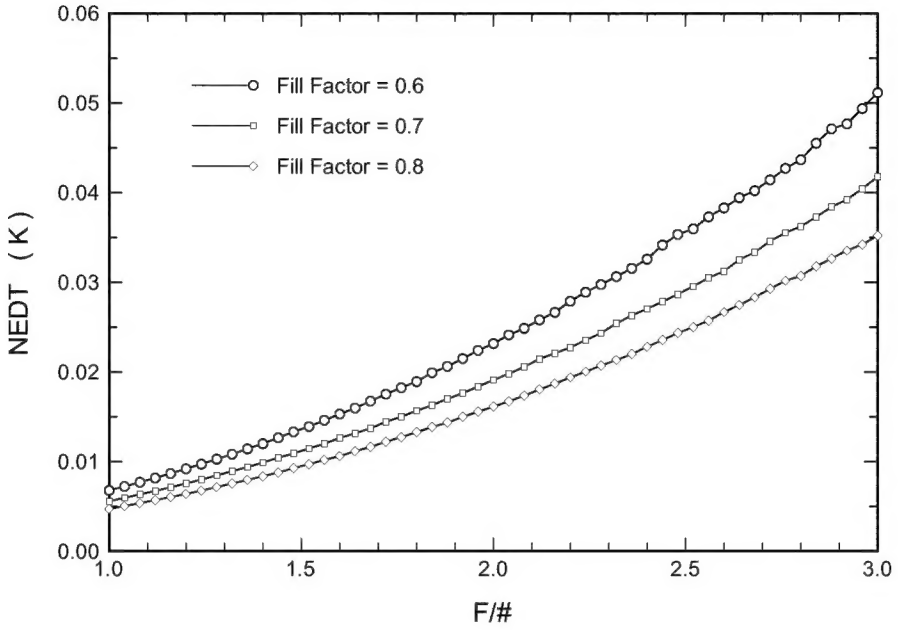

Fig. 6: Uncooled NEDT performance of a TTD 320x244 array with a 50x50 μm^2 pixel size, 0.36 eV barrier height, $5x10^{-8}$ W/K thermal conductivity, various fill factors, operating in the 8-14 μm band.

Fig. 7 illustrates the performance of the device at 400K using a 0.45 eV barrier. The NEDT has increased to 10 mK. The temperature coefficient is 4%/K. The total noise current is 4.24 x 10^{-19} A and the signal to noise ratio is 8,911. The doping concentration is $5x10^{15}cm^{-3}$ Since temperature stabilization by heating is 10-100 times more efficient than temperature stabilization by cooling military applications with high temperature operating environments may see significant power savings.

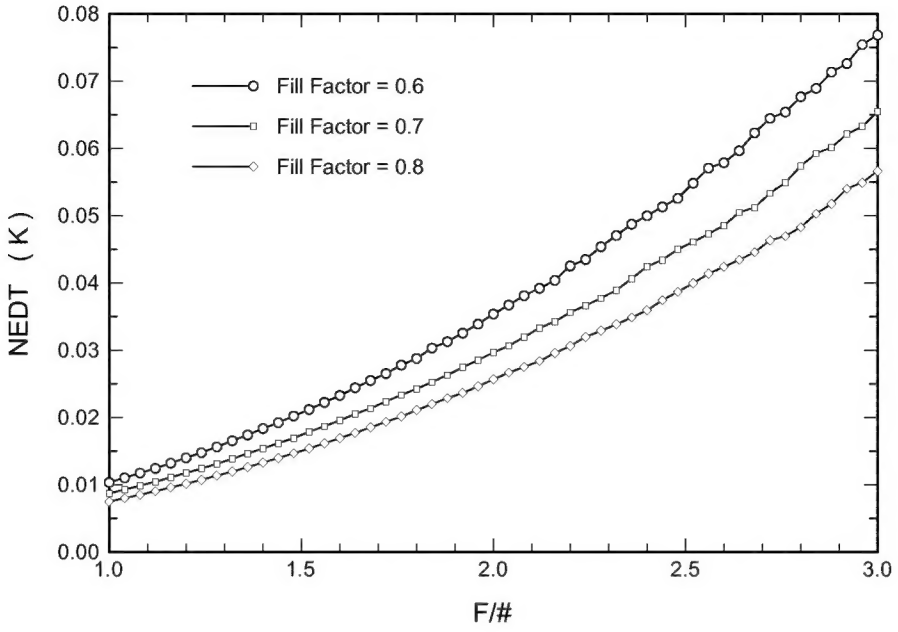

Fig. 7: Uncooled NEDT performance of a TTD 320x244 array with a 50x50 μm^2 pixel size, 0.45 eV barrier height, $5x10^{-8}$ W/K thermal conductivity, various fill factors, operating in the 8-14 μm band.

Fig. 8 demonstrates the effect increasing temperature on NEDT and the temperature coefficient (TC). Equations 4.7 and 6.7 were used to define TC and NEDT. The graph shows an increase in NEDT and a decrease in the temperature coefficient as a function of the operating temperature when holding the output current constant at 150μa. The increase in TC is approximately .025%/K. The decrease in NEDT is approximately .015mK/K. This allows a fairly accurate prediction of both NEDT and TC for various barrier heights and doping levels at a given temperature. For a doubling of temperature the corresponding change in NEDT and TC is roughly 50%.

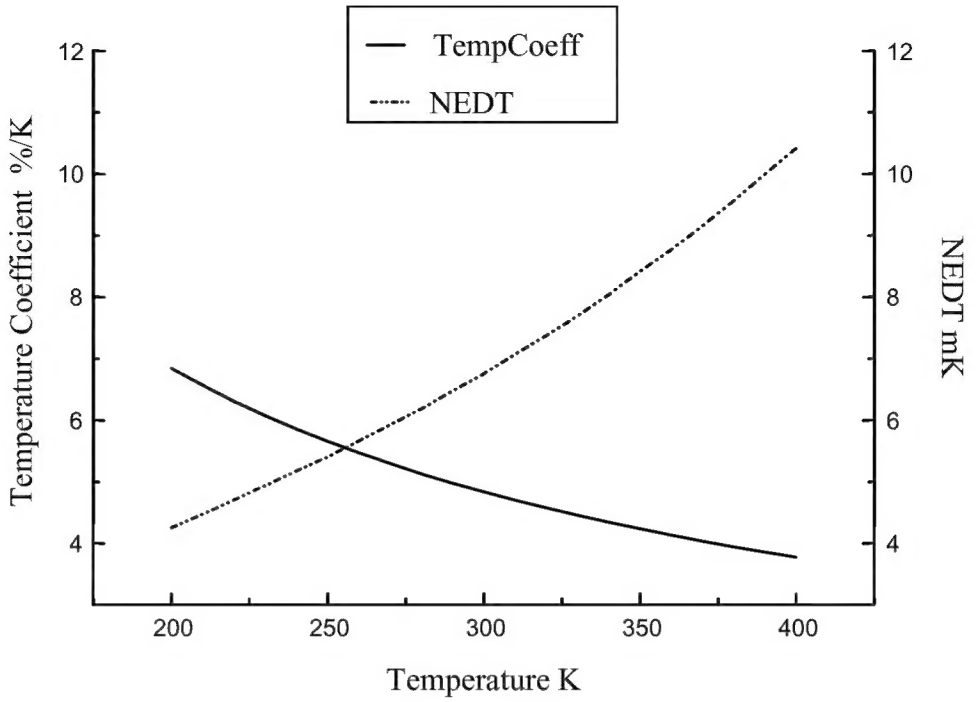

Fig.: 8 Temperature coefficient and NEDT of various barrier heights and doping levels as a function of temperature.

8. Conclusion

The operation of the TTD has been described in terms of the fundamental equations that govern its operation. They include a detailed description of the applicable optical, thermal and electrical equations that govern the operation of the TTD device element. These equations show the advantages and disadvantages of a Schottky barrier based TTD device element. The affect of the multiplexer and amplifier on the array has been considered along with the noise equivalent temperature (NEDT) of the array in terms of the equations derived in the previous sections. Additional simplifications were used to provide insight into the operation of the TTD. Finally, performance calculations for the TTD based on the above model were shown. Several additional observations regarding the operation of the TTD are worth noting: first, only 100-200 mV of reverse bias are required to sample the temperature of the detector. Consequently, sense element heating/cycling and the associated nonuniformities are expected to be minimal. Second, the dominant noise in a properly designed system is detector shot noise, hence the signal to noise ratio will improve as the square root of the signal current (the signal to noise ratio in the ideal resistor based microbolometer improves as the signal current). Third, temperature stabilization by heating is 10-100 times more efficient than temperature stabilization by cooling; consequently, military applications with high operating environments may see significant power savings. Finally, economies of scale in imager production are possible by using the same sensor system adjusted for the operating temperature by changing the sensing metal of the Schottky diode.

References

[1] Electronics: Microstructure Science, edited by N. Einspruch, "Formation and Characterization of Transition Metal Silicides," M. Nicolet and S. Lau, Academic Press, 1983, NY.

[2] Stratton T. G.,Cole B. E.,Kruse P. W., Wood R. A. et al., "High Temperature Superconducting Microbolometer," Appl. Phys. Lett 57(1), July 1990.

[3] Wood R. A. et al., "Uncooled Thermal Imaging with Monolithic Silicon Focal Plane Arrays," Proc. SPIE 2020, Infrared Technology XIX, 329, 1993.

[4] Johnson B. R., Kruse P. W., "Silicon Microstructure Superconducting Microbolometer Infrared Arrays," Proc. SPIE 2020, Infrared Technology XIX, 2-11, 1993.

[5] Choi J., Park Y. and Min H., "Extremely Thin SOI MOSFET Characteristics Including Inversion Layer to Accumulation Layer Tunneling" IEDM, 27.1.1, 1994.

[6] Keyes R. J., Optical and Infrared Detectors, Chapter 3, pp. 74, Springer Verlag, 1980.

[7] Sze S. M., Physics of Semiconductor Devices, Chapter 5, John Wiley & Sons, 1981.

[8] Sze S. M., Physics of Semiconductor Devices, pp 111-112, John Wiley & Sons, 1981.